

G. Röpke and A. Schnell¹Arbeitsgruppe "Quantenphysik und Vielteilchensysteme", FB Physik, Universität Rostock
Universitätsplatz 1, D-18051 Rostock, Germany

Correlation effects in nuclear matter at finite temperatures are studied for sub-nuclear densities ($\rho < \rho_0$) and medium excitation energy, where a nonrelativistic potential approach is possible. A quantum statistical approach is given, where clusters are treated under the influence of a clustered medium treated within a mean field approximation. Spectral functions, in-medium cross sections, and reaction rates are considered as well as the formation of a quantum condensate. In particular, exploratory calculations are shown with respect to the pseudo gap in the nucleon level density close to the superfluid phase transition. Estimates of isospin singlet pairing and quartetting in nuclear binding energies are given.

arXiv:nucl-th/9812027v1 10 Dec 1998

1 Introduction

Nuclear matter at finite temperature is an important prerequisite to understand the properties of not only ordinary nuclei but also excited nucleonic systems occurring for instance in heavy-ion collisions and astrophysical objects. Nuclear matter can be considered as a strongly interacting quantum liquid where the formation of correlations is a significant feature. In particular, a simple quasi-particle approach is not sufficient, rather one has to consider spectral functions in order to obtain off-shell information. We are treating equilibrium properties for mainly symmetric nuclear matter at medium excitation energies. We will concentrate on two-particle correlations.

We are considering nuclear matter as an infinite homogeneous system consisting of protons and neutrons. The hamiltonian H is given by

$$H = \sum_i \frac{\vec{p}_i^2}{2m_i} + \frac{1}{2} \sum_{i \neq j} V(\vec{r}_i - \vec{r}_j). \quad (1)$$

Such an approach is restricted to the nonrelativistic case. Different forms are known for the interaction potential V_{ij} which is derived from nucleon-nucleon (NN) scattering data. We will use the separable representations of the Paris and Bonn potential given by Plessas et al. [1, 2]

$$V_\alpha(p, p') = \sum_{i,j=1}^N w_{\alpha i}(p) \lambda_{\alpha i j} w_{\alpha j}(p'); \quad \text{uncoupled}, \quad (2)$$

$$V_\alpha^{LL'}(p, p') = \sum_{i,j=1}^N w_{\alpha i}^L(p) \lambda_{\alpha i j} w_{\alpha j}^{L'}(p'); \quad \text{coupled}. \quad (3)$$

Due to the interaction, bound states, scattering states as well as condensates are formed. The region of densities and temperatures where a many nucleon system can be described by the hamiltonian (1) is restricted to not too high densities ($\rho \leq \rho_0 = 0.17 \text{ fm}^{-3}$) and temperatures ($T \leq 30 \text{ MeV}$) (see Fig. 1). In this region, nuclear matter shows up interesting phenomena such as the liquid-gas type phase transition, the formation of bound states, and the transition to superfluidity.

2 Cluster mean field approximation

Different methods can be used to evaluate the properties of nuclear matter such as path integral, computer simulations and perturbation theory using a diagram representation for the thermodynamic Green's functions, which will be used here.

¹e-mail: arne@darss.mpg.uni-rostock.de

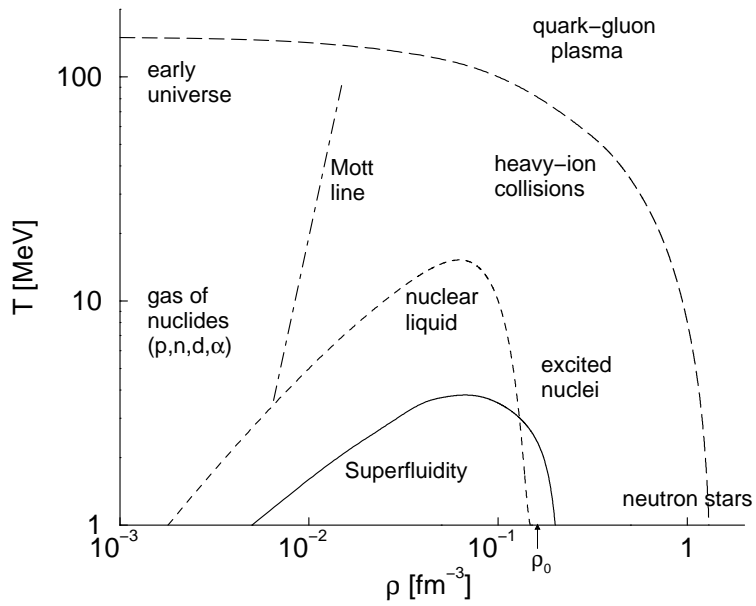


Figure 1: Schematic plot of the temperature-density plane of symmetric nuclear matter. The phase transition to the quark-gluon-plasma (dashed line) is hypothetical. Phase transitions strongly depend on isospin asymmetry.

Properties of the nucleonic many-particle system can be expressed in terms of the thermodynamic Green's function such as the equation of state [3] (p denoting momentum, spin, and isospin)

$$\rho(\beta, \mu) = \sum_p \langle a_p^+ a_p \rangle = \sum_p \int \frac{d\omega}{\pi} f(\omega) \text{Im} G(p, \omega - i0). \quad (4)$$

($f(\omega) = [\exp\{(\omega - \mu)/T\} + 1]^{-1}$ is the Fermi distribution function, μ the chemical potential, T the temperature.) The single-particle Green's function $G(p, z)$ is obtained from the self-energy $\Sigma(p, z)$ via the Dyson equation. To include correlations in the system, a cluster decomposition of the self-energy is performed in terms of n -particle contributions

$$\Sigma(1, z_\nu) = \text{Diagram } T_2 + \text{Diagram } T_3 + \dots \Big|_{\text{irred}}, \quad (5)$$

describing a n -particle cluster embedded in a mean field containing also the contributions of correlations [4, 5, 6]. In particular, we will concentrate on two-particle correlations. The ladder approximation for the two-particle T matrix is given by the Bethe-Salpeter equation

$$\text{Diagram } T_2 = \text{Diagram } K + \text{Diagram } K \text{ (ladder)} \quad (6)$$

The interaction kernel K contains, besides the potential V , also terms which describe the influence of the medium in consistency with the approximation made for the self-energy Σ (Ward identities). In particular, the one-particle Green's function is given in terms of the self-energy via the Dyson equation

$$\text{Diagram } G = \text{Diagram } G + \text{Diagram } T \quad (7)$$

For the calculation of the self-energy the two-particle Green's function has to be calculated as

$$\begin{array}{c}
 \boxed{G_2} = \begin{array}{c} \text{---} \rightarrow \\ \text{---} \rightarrow \end{array} \text{ex} + \begin{array}{c} \text{---} \rightarrow \\ \text{---} \rightarrow \end{array} \boxed{K} \boxed{G_2} \\
 = \begin{array}{c} \text{---} \rightarrow \\ \text{---} \rightarrow \end{array} \text{ex} + \begin{array}{c} \text{---} \rightarrow \\ \text{---} \rightarrow \end{array} \boxed{T} \begin{array}{c} \text{---} \rightarrow \\ \text{---} \rightarrow \end{array} .
 \end{array} \quad (8)$$

The interaction kernel K , which is related to the T matrix according to (6), is consistently given by

$$\boxed{K} = \begin{array}{c} \text{---} \rightarrow \\ \text{---} \rightarrow \end{array} + \begin{array}{c} \text{---} \rightarrow \\ \text{---} \rightarrow \end{array} \boxed{T} \begin{array}{c} \text{---} \rightarrow \\ \text{---} \rightarrow \end{array} \text{(2x)} + \begin{array}{c} \text{---} \rightarrow \\ \text{---} \rightarrow \end{array} \boxed{T} \begin{array}{c} \text{---} \rightarrow \\ \text{---} \rightarrow \end{array} \text{(2x)} + \begin{array}{c} \text{---} \rightarrow \\ \text{---} \rightarrow \end{array} \boxed{T} \begin{array}{c} \text{---} \rightarrow \\ \text{---} \rightarrow \end{array} \text{(2x)} .$$

The ordinary Hartree-Fock type approach is extended by including in Σ the two-particle correlations occurring in the medium but also, in a consistent manner, in K . The systematic account of n -particle correlations is denoted as cluster-mean field approximation. The correlations in the medium have to be determined in a self-consistent way [4, 5, 6].

In a simplified approach the equations above are not solved self-consistently, but treating the two-particle propagator in the Bethe-Salpeter equation for the T matrix on a quasi-particle level. Furthermore the Brückner approach is reproduced neglecting the contribution in K beyond V .

3 Two-particle properties in nuclear matter

Using the separable form of the potential (2), (3) an explicit solution of the Bethe-Goldstone equation in quasi-particle approximation can be given. Within a channel decomposition the following expressions for the T matrix can be given [3, 7, 8, 13]

$$T_{\alpha}^{LL'}(p, p', P, z) = \sum_{ijk} w_{\alpha i}^L(p) [1 - J^{\alpha}(P, z)]_{ij}^{-1} \lambda_{\alpha jk} w_{\alpha k}^{L'}(p') , \quad (10)$$

where the quantity J_{ij}^{α} (α denoting the interaction channel) is given by

$$J_{ij}^{\alpha}(P, z) = \int_0^{\infty} dp p^2 \sum_{nL} w_{\alpha n}^L(p) \lambda_{\alpha in} w_{\alpha j}^L(p) G_2^0(p, P, z) , \quad (11)$$

with the two-particle Green's function in quasi-particle approximation

$$G_2^0(p, P, z) = \frac{Q(p, P)}{\frac{p^2}{m} + \frac{P^2}{4m} + u(p, P) - z} . \quad (12)$$

$Q(p, P)$ and $u(p, P)$ are the angle-averaged Pauli blocking and single-particle potential, respectively, depending on relative (p) and total (P) momentum. From Eq. (10) one can easily identify the poles of the T matrix. Considering negative energies one obtains the following condition for the occurrence of a pole which describes in the ${}^3S_1 - {}^3D_1$ channel the deuteron bound state

$$\det[1 - \text{Re } J^{\alpha}(P, \omega = E_b(P) + E_{\text{cont}}(P))]_{ij} = 0 ; \quad (\alpha = {}^3S_1 - {}^3D_1) . \quad (13)$$

The solution of this equation is given in Fig. 2 where the in-medium binding energy E_b of the deuteron ($E_{\text{cont}}(P) = \frac{P^2}{4m} + u(0, P)$) is plotted for several values of the total momentum as a function of the

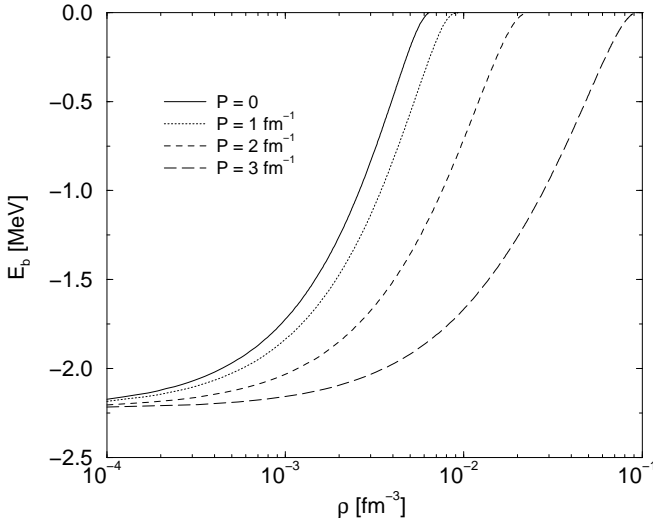


Figure 2: Deuteron binding energy in the nuclear medium as a function of the density for several total momenta. The calculation was done at $T = 10$ MeV temperature using the PEST4 potential (cf. [3]).

density. With increasing density the binding energy drops to zero at the so-called Mott density. This means that in the nuclear medium the deuteron is dissolved if the density is larger than approximately $\rho_0/20$. A finite total momentum leads to a shift of this Mott effect towards higher densities. Another quantity that can be derived from Eq. (10) is the in-medium NN scattering phase shift. It can be obtained by

$$\cot \delta_\alpha(\omega) = \frac{\text{Re } T(ppP, \omega)}{\text{Im } T(ppP, \omega + i0)} . \quad (14)$$

In Fig. 3 the phase shifts of the 1S_0 and the 3S_1 channel are given as a function of the energy for various densities at $T = 10$ MeV temperature. For very low densities the phase shifts approach the limit of free scattering. For higher densities the phase shifts are strongly modified in the low-energy region. In particular, one observes a jump of the 3S_1 phase shift at $\omega = 0$ from π to zero at approximately $\rho_0/20$. According to the Levinson theorem $\delta_\alpha(P, \omega = 0) = n\pi$ (n – number of bound states) this is due to the vanishing of the deuteron bound state at this density value.

4 One- and two-particle spectral function

The description of correlations in nuclear matter requires the knowledge of the full off-shell behavior of the nucleons. This information is contained in the spectral function of the nucleon. The solution of the two-particle problem can be used to improve the approximation for the spectral function. In this sense we go beyond the quasi-particle picture. The single-particle spectral function A_1 is calculated via the nucleon self-energy which itself is given by the T matrix in ladder approximation. It reads

$$A_1(p, \omega) = \frac{2\text{Im } \Sigma(p, \omega + i0)}{[\omega - p^2/(2m) - \text{Re } \Sigma(p, \omega)]^2 + [\text{Im } \Sigma(p, \omega + i0)]^2} . \quad (15)$$

In Fig. 4 the nucleon spectral function is displayed as a function of the energy and momentum [7]. The density is set to normal nuclear matter density $\rho_0 = 0.17$ fm $^{-3}$, the temperature is $T = 10$ MeV. For low momenta A_1 has a width of about 150 MeV which is quite large, particularly if compared to the δ -distribution of the quasi-particle spectral function. This can also be seen in Fig. 5 where the imaginary part of the self-energy is plotted as a function of the energy for various temperatures. At the chemical potential μ it exhibits a minimum which touches ground only for $T \rightarrow 0$. Another

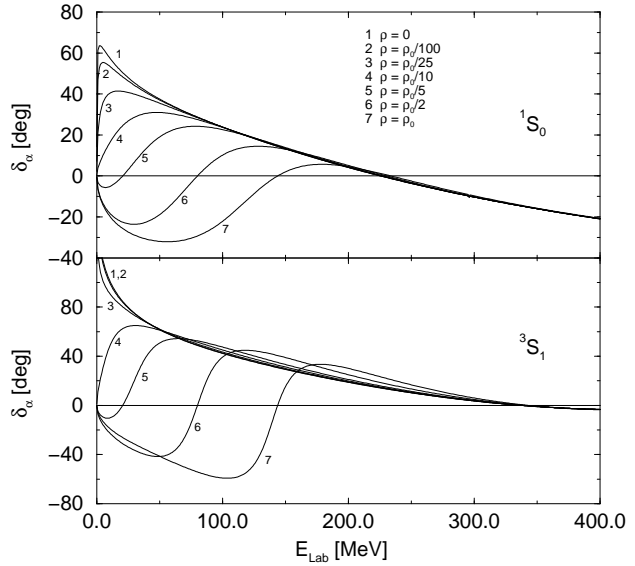


Figure 3: In-medium NN scattering phase shifts as a function of the lab energy for several values of the density at the temperature $T = 10$ MeV.

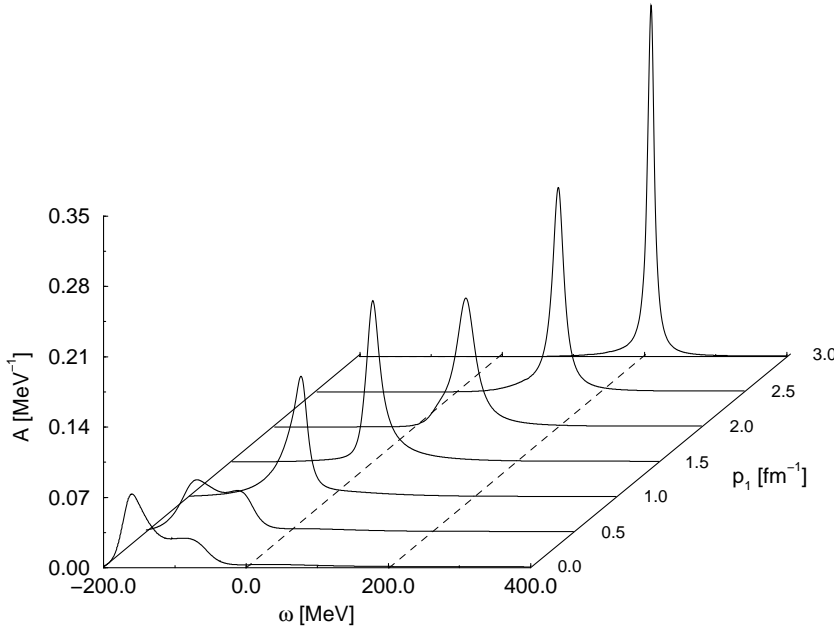


Figure 4: Nucleon spectral function as a function of the energy ω and momentum p_1 at the density $\rho = \rho_0$ and temperature $T = 10$ MeV [7]. The NN potential used is a separable form of the Paris potential [1].

At Fermi momentum one observes a Lorentz-like shape with a reduced but still considerable width. This is due to the fact that at finite temperatures the quasi-particles have finite life-time even at the Fermi surface.

interesting feature to be seen in Fig. 5 is the sharp peak at $\omega_0 = 2\mu - \epsilon(0)$ for the lowest temperature $T = 1.8$ MeV. It is a direct consequence of the pairing instability in the T matrix and therefore a precursor effect of the onset of superfluidity in nuclear matter which occurs at the critical temperature $T_c = 1.78$ MeV (see Sect. 6). From the spectral function one can easily obtain the nucleon momentum distributions via

$$n(p) = \int \frac{d\omega}{2\pi} f(\omega) A(p, \omega). \quad (16)$$

In Fig. 6 the momentum distribution is given for three values of the density and compared to the respective quasi-particle Fermi distribution functions. At low momenta one observes a depletion by about 10 to 15 percent, whereas for high momenta the momentum distribution is enhanced. This behavior is well known from electron scattering experiments (e,e'p) and due to nucleon-nucleon correlations. Similar investigations can be done for low-density nuclear matter where the deuteron bound state arises yielding an important contribution to the spectral function which cannot be described within a quasi-particle model [8].

In Section 3 it has been demonstrated that the deuteron bound state as well as scattering states play an important role in low-density nuclear matter. Similar to the description of single-particle states the two-particle spectral function is the appropriate tool for two-particle states. It is defined by the imaginary part of the two-particle Green's function $a_2(p_1 p_2 p'_1 p'_2, \omega) = \text{Im } G_2(p_1 p_2 p'_1 p'_2, \omega)$ and can be also calculated via the ladder T matrix. In order to have the spectral function as function of total momentum and energy at our disposal and for practical purposes we define

$$A_2(P, \omega) = \sum_{pp'} w(p) a_2(P/2 + p, P/2 - p, P/2 + p', P/2 - p', \omega) w(p'). \quad (17)$$

which is an average with respect to the relative momenta retaining the important informations. Of particular interest is the behavior of A_2 close to the superfluid phase transition. In contrast to BCS theory, which can be applied above and below T_c , but is based on quasi-particle concepts, the standard T matrix approach includes correlations, but cannot be extended to describe superfluid nuclear matter.

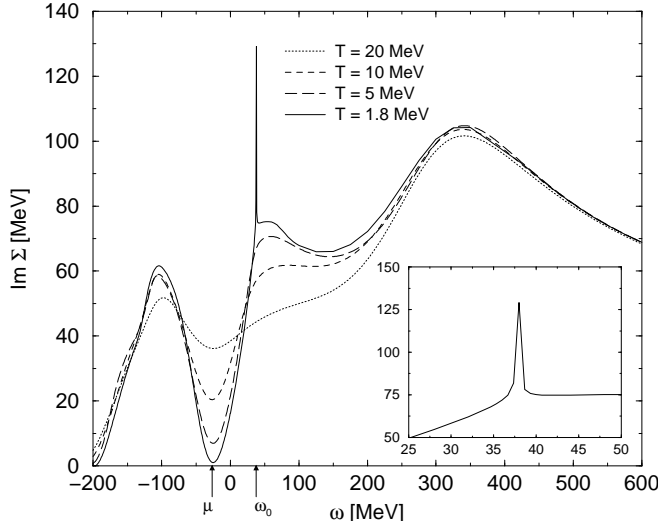


Figure 5: Imaginary part of the self-energy as a function of the energy for several temperatures at a fixed density $\rho = \rho_0$. The momentum was set to zero. The critical temperature for the onset of superfluidity is $T_c = 1.78$ MeV.

As a first step to overcome this deficiency we investigate the precritical behavior of the level density

$$N(\omega) = \sum_p \delta(\omega - \epsilon(p)), \quad (18)$$

which is given by the real part of the nucleon self-energy and implicitly by the two-particle spectral function

$$\epsilon(p) = \frac{p^2}{2m} + U(p); \quad U(p) = \text{Re } \Sigma(p, \epsilon(p)). \quad (19)$$

The real part of the self-energy can be cast in the following form

$$\text{Re } \Sigma(p_1, \epsilon(p_1)) = \sum_2 f(\epsilon_2) \text{Re } T(p_1 p_2 p_1 p_2, \epsilon_1 + \epsilon_2) + \sum_2 \int \frac{d\omega}{\pi} g(\omega) \frac{\text{Im } T(p_1 p_2 p_1 p_2, \omega + i0)}{\omega - \epsilon_1 - \epsilon_2}. \quad (20)$$

In Fig. 7 the level density is given as a function of the energy for two temperatures. At $T = 6$ MeV (close to the critical temperature of the superfluid phase transition) the level density exhibits a pre-critical pseudo gap which has the size of the BCS gap at $T = 0$. This means, that the onset of superfluidity does not happen sharply at T_c signaled by the spontaneous opening of a gap in the level density as supposed by BCS theory. Rather, due to strong correlations, a soft transition to superfluidity with the formation of a pseudo gap can be observed. It is therefore necessary to go beyond the mean field approach of the BCS-theory and to generalize the T matrix approximation to below T_c .

5 In-medium cross sections

Another important quantity that can be derived from the two-particle T matrix is the cross section of elastic nucleon-nucleon scattering. It can be assumed that the scattering process will be strongly modified in the nuclear medium due to phase space occupation and mean field effects. This is of particular interest for the simulation of heavy-ion collisions by transport codes (BUU, QMD) where the NN cross section is an important input quantity. In terms of the T matrix it reads

$$\sigma_T(P, \omega, \mu, T) = \frac{4\pi}{p^2} \frac{N^2(\omega, P)}{(2s_1 + 1)(2s_2 + 1)} \sum_{JLL'} (2J + 1) |T_{\alpha}^{LL'}(p, P, \omega)|^2 \quad (21)$$

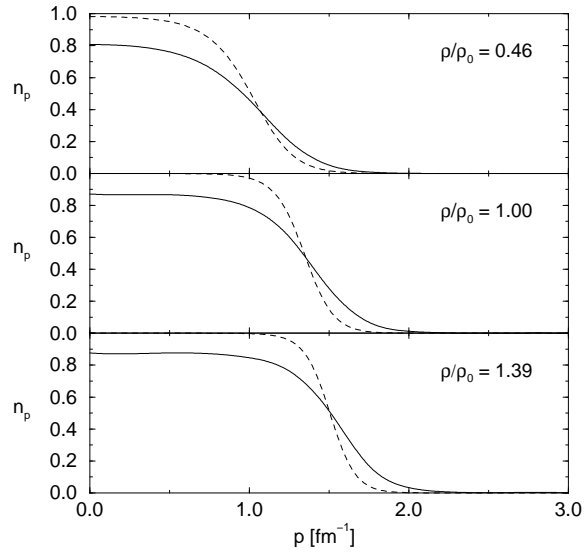


Figure 6: Nucleon momentum distribution for three values of the density for the temperature $T = 10$ MeV. The dashed curves represent the ideal Fermi gas.

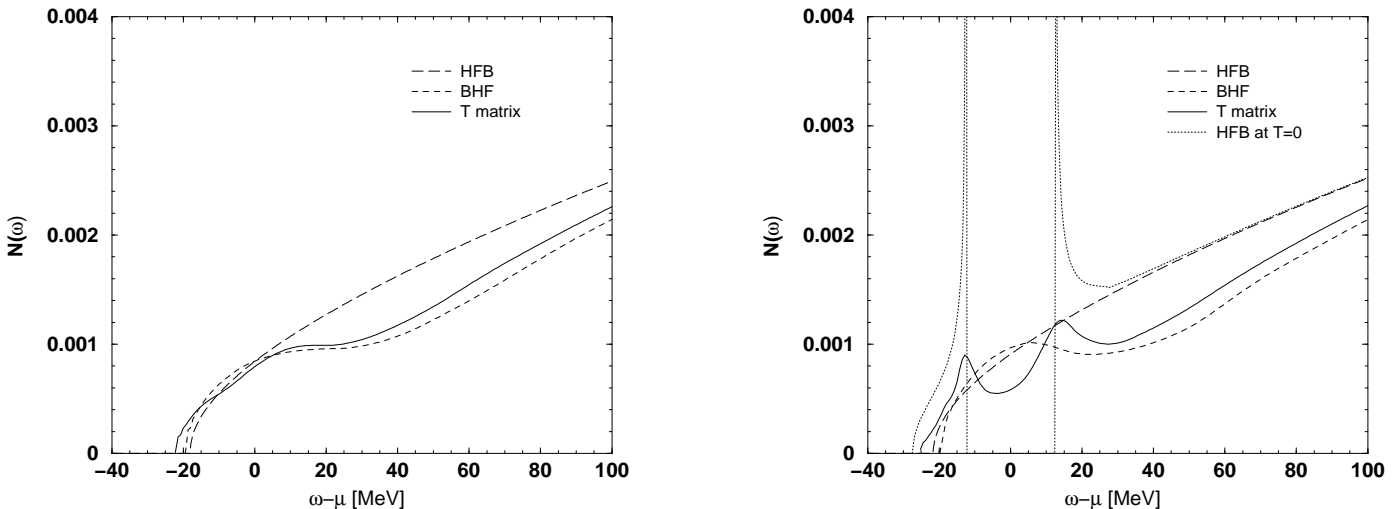


Figure 7: Nucleon level density $N(\omega)$ as a function of $\omega - \mu$ (μ – chemical potential) at the density $\rho = \rho_0/3$ for different approximations (HF-Bogoliubov, Brückner-HF, T matrix approach). Left: Temperature $T = 10$ MeV, far above the critical temperature; Right: Temperature $T = 6$ MeV, close to the critical temperature. For comparison the BCS solution at $T = 0$ is given by the dotted curve.

with the generalized density of states $N(\omega, P)$ and the angle-averaged two-particle energy $\epsilon(p, P)$ (for details see [9]). The in-medium total NN cross section is then given by $\sigma_{NN} = \frac{1}{2} [\sigma_{pp} + \sigma_{pn}] = \frac{1}{4} [\sigma_0 + 3\sigma_1]$. In order to reduce the number of variables we use an average procedure according to collisional integral (loss term) of the Boltzmann equation given by

$$\begin{aligned} \langle \sigma \rangle_{NN}(p_1) &= \frac{1}{\langle N \rangle} \int d^3 p_2 f(p_2) Q_{pp}(p, P) \frac{\sigma_{NN}[\epsilon(p, P), P]}{N[\epsilon(p, P), P]} \\ Q_{pp}(p, P) &= \int \frac{d\Omega}{4\pi} [1 - f(p_1)] [1 - f(p_2)], \quad \langle N \rangle = \int d^3 p_2 \frac{f(p_2)}{N[\epsilon(p, P), P]}. \end{aligned} \quad (22)$$

We obtain an average over the occupation of the final states weighted with the relative velocity of the particles. Figure 8 shows in the upper panels the average cross section as a function of the momentum p_1 for various densities and temperatures. The thin lines represent the calculation of Eq. (22) using the free cross section instead of the in-medium quantity. All other quantities in (22) remain the same and therefore the 'free' average cross section $\langle \sigma \rangle_{\text{free}}$ depends on density and temperature. It demonstrates simply the influence of the in-medium cross section compared to the free one, which can be seen in the lower panels of Fig. 8 where the ratio $\langle \sigma \rangle_{NN}/\langle \sigma \rangle_{\text{free}}$ is given. The density dependence of this ratio is shown in Fig. 9 for various scattering energies and temperatures. The in-medium cross section is strongly reduced with increasing density, in particular for lower scattering energies. The temperature dependence is rather weak. The parabolic density dependence can be easily parametrized as well as the dependence on energy and temperature (see [9]).

In heavy-ion collisions not only two-particle states are of relevance, also three particle processes such as the deuteron formation and break-up play a significant role. In order to improve the mean-field treatment of the two-particle problem in nuclear matter, the three-particle problem in matter can be considered. In addition to the broadening of the bound state levels, also reaction rates for break-up and formation of deuterons can be obtained. A Faddeev-type AGS equation has been solved, where the influence of the medium on the three-particle system was considered in mean-field approximation [10]. As a result an increase of the deuteron break-up and formation rates has been obtained due to the influence of the medium.

6 Superfluidity in nuclear matter

Another highly interesting phenomenon in nuclear matter is the occurrence of pairing effects. One distinguishes between isospin triplet pairing ($S = 0, T = 1$) which is known from even-odd staggering

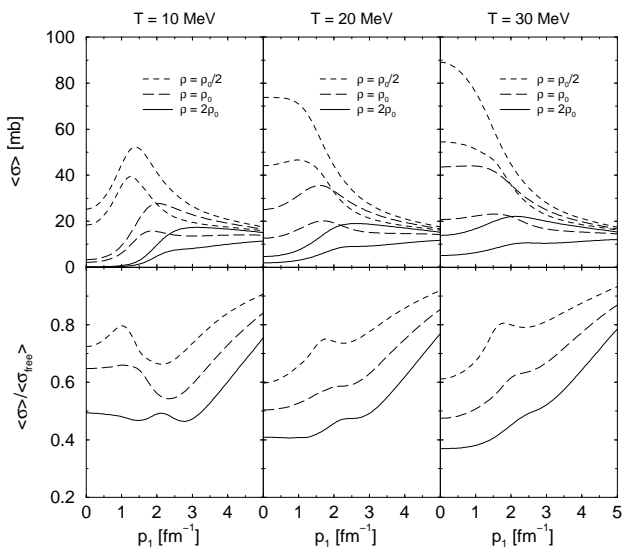


Figure 8: Average cross section as function of the momentum p_1 for three values of temperature and density, respectively. Upper half: Absolute values of the average free (thin lines) and in-medium (thick lines) cross sections. Lower half: ratio of in-medium vs. free average cross section.

of nuclear binding energies and isospin singlet pairing ($S = 1, T = 0$) which, however, cannot so easily be identified in nuclear structure systematics. The reason for this could be the fact that nuclei along the stability line are isospin asymmetric and therefore protons and neutrons have different chemical potentials. It has been shown in nuclear matter calculations [12] that asymmetry destroys isospin singlet pairing very effectively. In the following we discuss only this kind of pairing in connection with the formation of a superfluid phase in symmetric nuclear matter. For this reason we consider the pole of the T matrix describing the Cooper pairs

$$\det[1 - \text{Re } J^\alpha(\mu, T = T_c, P, \omega = 2\mu)]_{ij} = 0. \quad (23)$$

It defines the critical temperature T_c of the superfluid phase transition which is a function of the chemical potential (related to the density via the equation of state) and the total momentum. Using a generalized Beth-Uhlenbeck approach [3] where the total density is composed of free (quasi-particle) and correlated (bound and scattering) particles ($n_{\text{tot}} = n_{\text{free}} + 2n_{\text{corr}}$), the critical temperature T_c is calculated from (23) as shown in Fig. 12. Furthermore, the composition ratio $n_{\text{corr}}/n_{\text{tot}}$ is given as a function of the total density and the temperature [13]. In Fig. 13 T_c is compared to two limiting approximations. For low densities deuterons can exist (as we have seen previously) and form a Bose-Einstein condensate below the critical temperature. Treating the deuterons as ideal Bose system results in the long-dashed curve which is reached at very low density. At high densities correlation effects are small (see Fig. 12) and we can consider the independent particle model by introduction of BCS quasi-particles. The result is given as the short-dashed curve which is reached at high densities. The transition between both limiting cases is smooth and was first investigated by Nozières and Schmitt-Rink [14].

Besides the two-particle pairing discussed so far, a possible four-particle condensation (quartetting) may also play an important role in nuclei as well as during the expansion phase of heavy-ion collisions or in astrophysical objects. We estimate the onset of quartetting in nuclear matter by the solution of the following effective four-particle wave equation

$$\Psi_4(1234) = \sum_{1'2'3'4'} K_4(1234, 1'2'3'4', 4\mu) \Psi_4(1'2'3'4'), \quad (24)$$

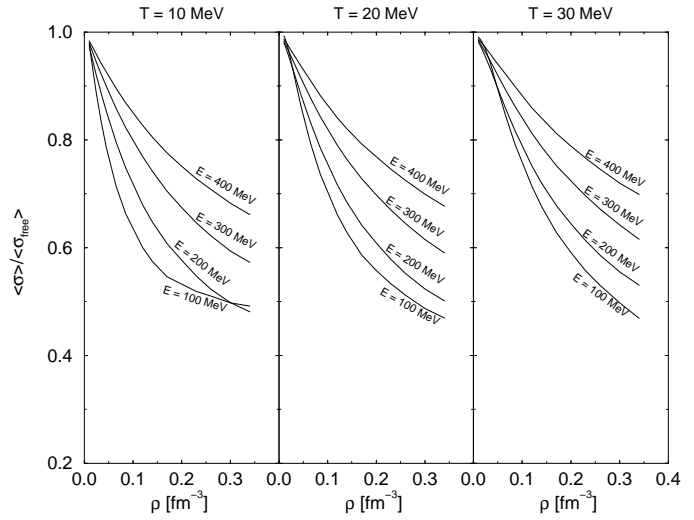


Figure 9: Ratio of the in-medium vs. free average cross section as function of the density ρ for three different temperatures and several values of the scattering energy $E = p_1^2/(2m)$.

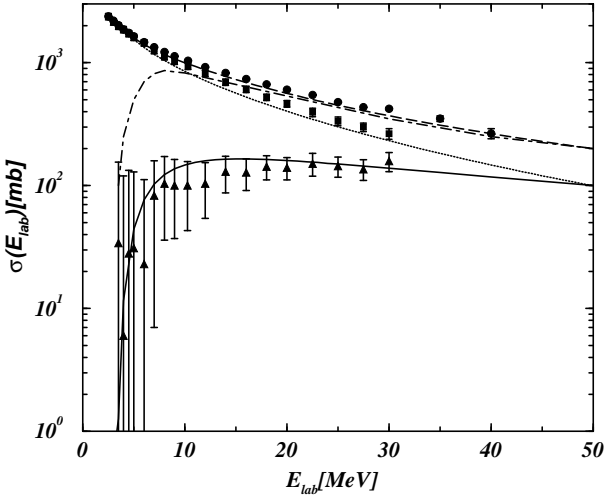


Figure 10: Neutron-deuteron cross section in nuclear matter (Data from [11]).

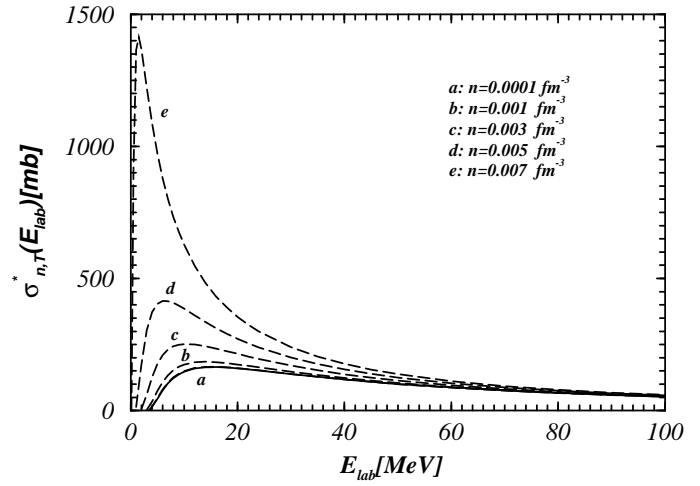


Figure 11: Medium dependence of the break-up $n-d$ cross section, temperature $T = 10$ MeV [10].

with the four-particle interaction kernel

$$K_4(1234, 1'2'3'4', z) = V(12, 1'2') \frac{f(1)f(2)}{g_2(12)} \frac{\delta_{33'}\delta_{44'}}{z - E_4(1234)}. \quad (25)$$

We use the variational calculation ansatz of the wave function Ψ_4

$$\Psi_4(1234) = \phi((\vec{p}_1 - \vec{p}_2)/2)\phi((\vec{p}_3 - \vec{p}_4)/2)\psi(\vec{p}_1 + \vec{p}_2) \quad (26)$$

optimizing the quasi-deuteron wave functions (ϕ) building the α -particle with a Gaussian ansatz for the relative motion between pairs (ψ)

$$\Psi_4(1234) = \phi((\vec{p}_1 - \vec{p}_2)/2)\phi((\vec{p}_3 - \vec{p}_4)/2)\psi(\vec{p}_1 + \vec{p}_2). \quad (27)$$

The results of this calculation are given in Fig. 14 where the critical temperatures of quartetting is given as a function of the chemical potential (left) and the uncorrelated density (right) [15]. Additionally, the pairing curves are given as dashed lines.

7 Isospin singlet pairing in nuclei

Finally we come now to the question whether it is possible to find signatures of isospin singlet pairing and quartetting in the systematics of nuclear binding energies. Empirically, the binding energy of nuclei can be decomposed according to the Bethe-Weizsäcker formula

$$\begin{aligned} B(Z, N) = & B_{\text{bulk}}(Z, N) + B_{\text{surf}}(Z, N) + B_{\text{Coul}}(Z, N) + B_{\text{asym}}(Z, N) \\ & + B_{\text{shell}}(Z, N) + B_{\text{pair}}(Z, N) + \Delta B(Z, N) \end{aligned} \quad (28)$$

which contains the main contributions including B_{pair} for $T = 1$ pairing. The additional term $\Delta B(Z, N)$ contains among others the effects of correlations between protons and neutrons, both isospin singlet pairing and quartetting. We represent $\Delta B(Z, N)$ as a function of the asymmetry $N - Z$

$$\begin{aligned} \Delta B(Z, N) = & b_0(Z)\delta_{Z,N} + b_1(Z)\delta_{Z,N+1} + b_{-1}(Z)\delta_{Z,N-1} + b_2(Z)\delta_{Z,N+2} + b_{-2}(Z)\delta_{Z,N-2} + \dots \\ = & \sum_i b_i(Z)\delta_{Z,N+i} \end{aligned} \quad (29)$$

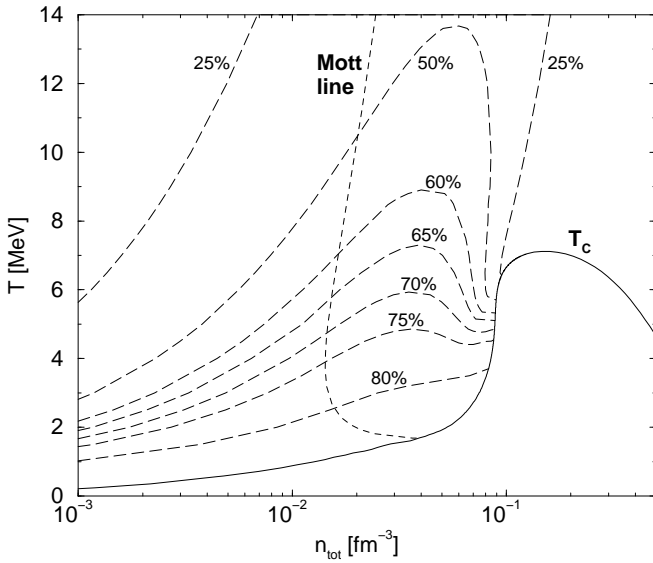


Figure 12: Composition of nuclear matter in the density-temperature plane calculated in the generalized Beth-Uhlenbeck approach using the Yamaguchi potential. The long-dashed curves are lines of equal concentration of correlated pairs. The Mott line indicates the deuteron break-up due to Pauli blocking.

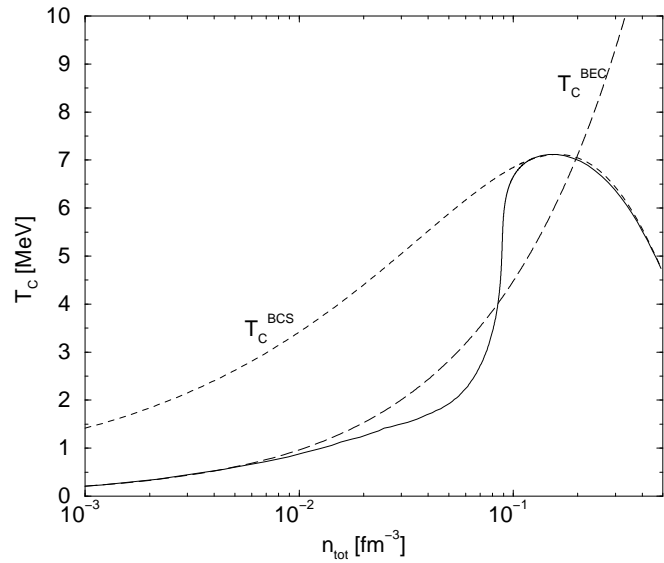


Figure 13: Critical temperatures of the onset of superfluidity as a function of the total density. The Beth-Uhlenbeck approximation shows a smooth transition from Bose-Einstein condensation of deuterons at low densities (long-dashed curve) to BCS pairing at high densities (short-dashed curve).

Now the question arises how to extract $\Delta B(Z, N)$ from experimental binding energies. For this purpose we define several types of filters which can be used to cancel the main contributions of (28) leaving only the term of interest. The horizontal and vertical filters

$$h(Z, N) = 2B(Z, N) - B(Z, N-2) - B(Z, N+2) - 2B(Z-2, N) + B(Z-2, N-2) + B(Z-2, N+2), \quad (30)$$

$$v(Z, N) = 2B(Z, N) - B(Z-2, N) - B(Z+2, N) - 2B(Z, N+2) + B(Z-2, N+2) + B(Z+2, N+2) \quad (31)$$

are differences of second order and the smallest filters possible. Other filters can be constructed using h and v such as

$$W(A) = -\frac{1}{8}v\left(\frac{A}{2}, \frac{A}{2}-2\right) - \frac{1}{8}h\left(\frac{A}{2}, \frac{A}{2}-2\right), \quad (32)$$

which is the type of filters Satula and Wyss used [16], or

$$g(Z, N) = \frac{1}{8}h(Z, N) - \frac{1}{8}h(Z+2, N), \quad (33)$$

which is the most symmetric filter. We will concentrate here only on the h -filter. In Fig. 15 $h(Z, Z+i)$ is given for even-even nuclei. From this and from odd-odd and odd-even/even-odd nuclei, which are not displayed here, one can derive the following features: (i) $h(Z, Z) \approx -h(Z, Z-2)$, (ii) $h(Z, Z-1) \approx 0$, and (iii) $h(Z, Z+i) \approx 0$ for $i > 3$. Based on these properties we can make assumptions which are necessary to find a solution of the following equation

$$h(Z, N) = -b_{N-Z-2}(Z) + 2b_{N-Z}(Z) + b_{N-Z}(Z-2) - b_{N-Z+2}(Z) - 2b_{N-Z+2}(Z-2) + b_{N-Z+4}(Z-2) \quad (34)$$

which relates the filter h to the coefficients b_{N-Z} of Eq. (29). Using $b_i(Z-2) \approx b_i(Z)$ results in

$$h(Z, N) \approx -b_{N-Z-2}(Z) + 3b_{N-Z}(Z) - 3b_{N-Z+2}(Z) + b_{N-Z+4}(Z). \quad (35)$$

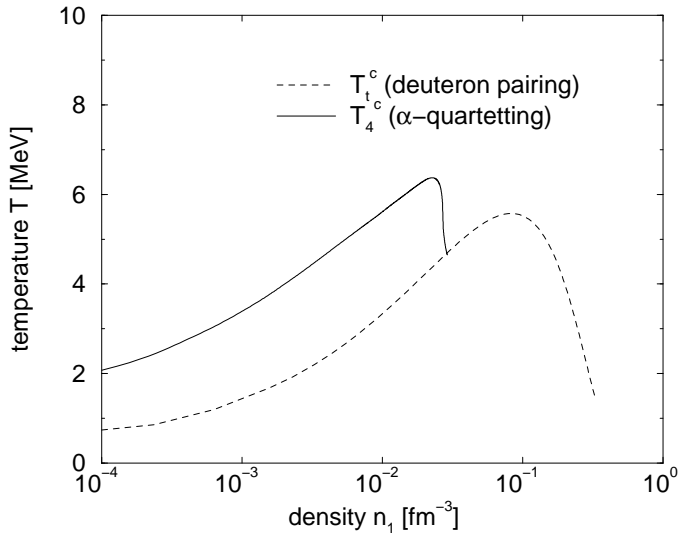
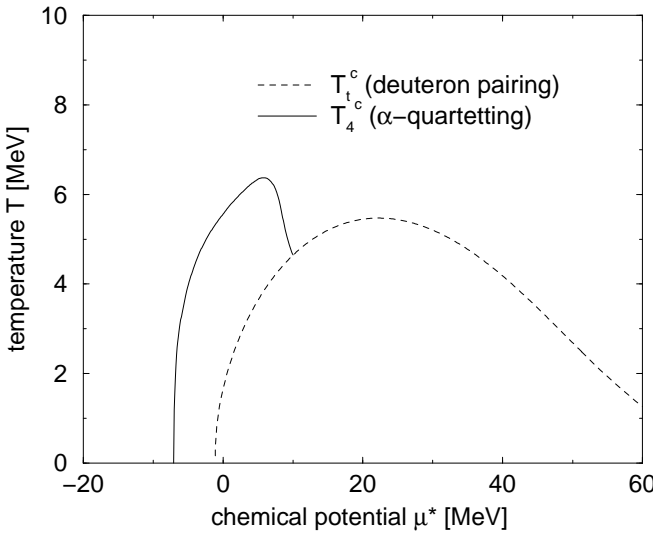


Figure 14: Critical temperatures for the onset of quantum condensation in symmetric nuclear matter, model calculation [15]. The critical temperature of the onset of two-particle spin triplet pairing T_t^c is compared with T_4^c for the onset of a four-particle condensate. The left-handed figure shows the behavior as a function of the chemical potential, the right-handed figure as a function of the uncorrelated density.

$b_i(Z) \approx b_{|i|}(Z)$ reproduces property (i) and (ii), and $b_i \equiv 0$ for $|i| \geq 6$ is a consequence of property (iii). By means of the results of $h(Z, Z + i)$ ($i = 0, 1 \dots 5$) one can solve the system of equations (35) and obtains $b_i(Z)$. The average of $b_i(Z)/b_0(Z)$ over the proton number Z is displayed in Fig. 16 in dependence of the asymmetry parameter $|N - Z|$. With increasing asymmetry the parameter b_{N-Z} drops to zero rather quickly. The contribution of proton-neutron or α correlations Δ can therefore be assumed to become small with increasing isospin asymmetry as it is expected from nuclear matter calculations. The contributions of isospin singlet pairing to nuclear binding energies can be estimated within a local density approximation. Based on results for the gap energy in asymmetric nuclear matter further studies are in progress. The contribution of quartetting can be estimated to be of the order of approximately 0.2 MeV for symmetric nuclei with $A \approx 100$, see [15].

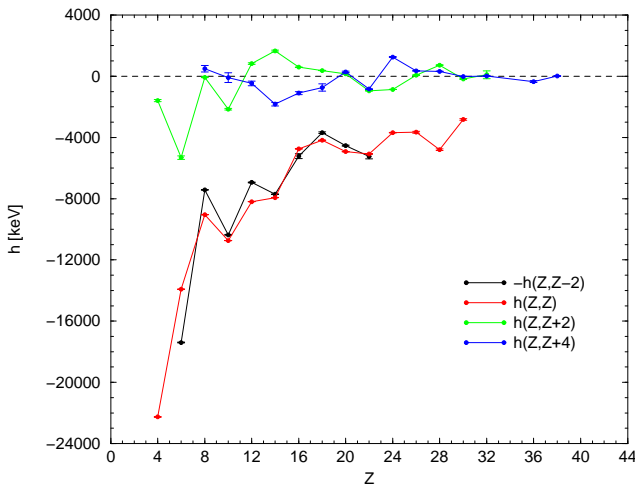


Figure 15: The filter $h(Z, Z + i)$ for even proton number Z and $i = -2, 0, 2, 4$ considering only even-even nuclei.

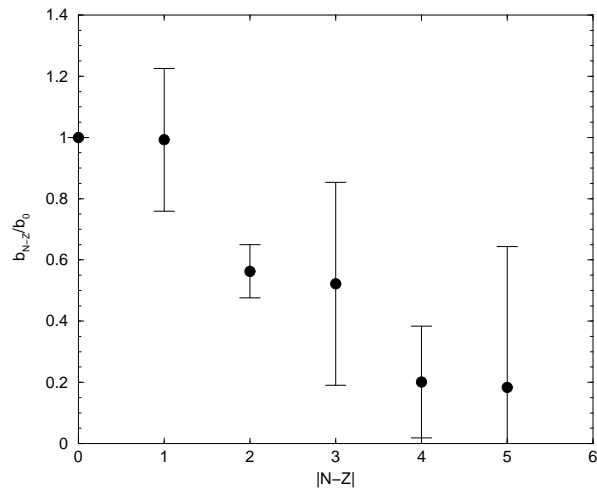


Figure 16: The average of the ratio b_{N-Z}/b_0 as a function of the absolute value of the proton-neutron difference as it is derived from the filter h .

8 Conclusions

We have shown that nuclear matter is an interesting example of a strongly coupled fermion system. In the region of subnuclear densities ($\rho_0/100 \leq \rho \leq \rho_0$) and several MeV temperature strong correlations occur leading to a variety of in-medium effects which cannot be explained in terms of a quasi-particle concept. The appropriate description can be given by spectral functions of the nucleon or even higher clusters. Two-particle properties, such as the binding energy of the deuteron, scattering phase shifts and the nucleon-nucleon or deuteron break-up cross section are strongly modified in the nuclear medium. Taking these into account will lead to different predictions concerning transport properties in nuclear collisions like nuclear flow or abundancies of mass fragments. The appearance of quantum condensates in nuclear matter is another exciting topic. The inclusion of correlations leads to significant precursor effects of the superfluid phase transition above T_c . Great effort has to be done to generalize the T matrix approach to describe the equation of state also for the region below T_c .

References

- [1] J. Haidenbauer and W. Plessas, Phys. Rev. C **30**, 1822 (1984).
- [2] Plessas et al., Few-Body Syst. Suppl. **7**, 251 (1994).
- [3] M. Schmidt, G. Röpke, and H. Schulz, Ann. Phys. (N.Y.) **202**, 57 (1990).
- [4] G. Röpke, L. Münchow, and H. Schulz, Nucl. Phys. **A379**, 536 (1982); Nucl. Phys. **A399**, 587 (1983).
- [5] G. Röpke, Ann. Phys. **3**, 145 (1994); Z. Phys. B **99**, 83 (1995).
- [6] J. Dukelsky, G. Röpke, and P. Schuck, Nucl. Phys. **A628**, 17 (1998).
- [7] T. Alm, A. Schnell, G. Röpke, N. Kwong, and S. H. Köhler, Phys. Rev. C **53**, 2181 (1996); Schnell, T. Alm, and G. Röpke Phys. Lett. B **387**, 443 (1996).
- [8] T. Alm, A. Schnell, and H. Stein, and G. Röpke, Phys. Lett. B **346**, 233 (1995).
- [9] H.-J. Schulze, A. Schnell, G. Röpke, U. Lombardo, Phys. Rev. C **56**, 3006 (1997); A. Schnell, G. Röpke, U. Lombardo, H.-J. Schulze, Phys. Rev. C **57**, 806 (1998).
- [10] M. Beyer, G. Röpke, and A. Sedrakian, Phys. Lett. B **376**, 7 (1996); M. Beyer and G. Röpke, Phys. Rev. C **56**, 2636 (1997).
- [11] P. Schwarz et al., Nucl. Phys. **A201**, 261 (1973).
- [12] T. Alm, B. L. Friman, G. Röpke, and H. Schulz, Nucl. Phys. **A551**, 45 (1993); T. Alm, G. Röpke, A. Sedrakian, and F. Weber, Nucl. Phys. **A604**, 491 (1996).
- [13] T. Alm, G. Röpke, A. Schnell, and H. Stein, Z. Phys. A **351**, 295 (1995).
- [14] P. Nozières and S. Schmitt-Rink, J. Low Temp. Phys. **59**, 159 (1985).
- [15] G. Röpke, A. Schnell, P. Schuck, and P. Nozières, Phys. Rev. Lett. **80**, 3177 (1998).
- [16] W. Satula and R. Wyss, Phys. Lett B **393**, 1 (1997); W. Satula, D.J. Dean, J. Gary, S. Mizutori, and W. Nazarewicz, Phys. Lett B **407**, 103 (1997).